Check for updates

A CFD modeling procedure to assess the effect of wind in settling tanks

A. Gkesouli and A. Stamou

ABSTRACT

We propose a systematic procedure that combines computational fluid dynamics (CFD) modeling and experimental work to answer two research questions that are usually posed by researchers and managers of water treatment plants: 'Is the effect of wind on settling tanks important?' and 'How can we determine this effect in our settling tanks?' We apply this procedure in the water treatment plant of Aharnes, Athens to derive the following conclusions. (1) The effect of wind increases with increasing co-current wind velocity, increasing settling velocity and decreasing flow rate. (2) In windy steady-state flow conditions, the degree of complexity and three-dimensionality of the flow field that is observed in calm conditions is reduced and the removal efficiency decreases from 85.1 in calm conditions to 82.0%. Predicted efficiencies for constant and variable inlet solids' concentrations compare favorably with measurements. (3) In windy, transient flow conditions, field data show that the effect of wind on the tank's efficiency can be very pronounced and within the first half hour of the windy period the efficiency decreases to approximately 55%; the present model does not capture this effect, because it cannot simulate the sludge layer and the subsequent re-suspension of the settled solids.

Key words | computational fluid dynamics, settling tanks, water treatment plants, wind effect

A. Gkesouli (corresponding author)
A. Stamou
Laboratory of Applied Hydraulics, Department of Water Resources and Environmental Engineering, School of Civil Engineering, National Technical University of Athens, Iroon Polytechniou 5, 15780 Athens, Greece
E-mail: *anthi.gkesouli@gmail.com*

INTRODUCTION

Sedimentation is a physical treatment process that is widely applied in water and wastewater treatment. In conventional water treatment plants (WTPs), the most widely applied treatment technology combines four processes: coagulation, sedimentation, filtration, and disinfection. Sedimentation takes place into the so-called settlings tanks, in which a significant percentage of suspended solids (*SS*) that is formed by the aggregation of particles of the untreated water with flocculants in the upstream coagulation units, settles by gravity and therefore influences the degree of treatment of the downstream units and the efficiency of the plant. The most important characteristic of a settling tank is its removal efficiency, which depends on the characteristics of the untreated water, such as the flow rate and the composition-concentrations of *SS*, the characteristics of the tank, such as its geometry including its inlet and outlet structures and the hydrodynamics, and the environmental characteristics, mainly the wind characteristics. There have been numerous studies on the determination of the effect of the above-mentioned factors that influence the hydraulic or the removal efficiency of settling tanks, which are theoretical, experimental, or numerical (e.g., Deininger *et al.* 1998; Stamou *et al.* 2000; Al-Sammarraee & Chan 2009).

Practically, all performed studies dealt with the effect of the characteristics of the untreated water or the characteristics of settling tank on the tank's efficiency, while the effect of the wind has always been neglected, although it is generally recognized that the operation of settling tanks is

doi: 10.2166/hydro.2018.048

Downloaded from http://iwaponline.com/jh/article-pdf/21/1/123/658230/jh0210123.pdf
by guest

sensitive to wind effects (Abdel-Gawad & McCorquodale 1985; Matko *et al.* 1996; Goula *et al.* 2008; Jover-Smet *et al.* 2017) and this should be taken into account in their design (Kawamura 2000). Moreover, troubleshooting guidelines for managers and operators of treatment plants (Florida Rural Water Association 2005) suggest that settling tanks should be checked for wind currents and, if required, the operators may install protection baffles. We can explain practically the effect of the wind assuming a long rectangular settling tank that is aligned co-currently with the wind, which has an inlet in its beginning and an outlet at its far end, such as the tank in Figure 1(a). The strong wind causes waves and high flow velocities at the water surface and creates the typical two-layer wind-induced flow field which consists of a strong surface current towards the outlet and a return current (towards the inlet) along the bottom (Stamou & Gkesouli 2015; Gkesouli *et al.* 2016). In other words, the flow in the tank is governed by a massive recirculation region occupying practically the whole tank which increases the degree of turbulence and mixing and, thus, hinders settling and reduces the efficiency of the tank (Ekama & Marais 2004). Moreover, the strong surface current drives the water fast towards the outlet where high flow velocities are observed and, thus, high surface loadings, creating significant short-circuiting (Crittenden *et al.* 2012), i.e., significant reduction of the retention time (Khezri *et al.* 2012), while the high flow velocities in the bottom upstream current create re-suspension of the settled solids and their accumulation in the tank (Aalderlink *et al.* 1984), thus, reducing the tank's efficiency. For the above-mentioned orientation of the tank, the negative effects are more pronounced when the length of the tank is longer than 30 m (Crittenden *et al.* 2012). It is noted that very rarely (practically never) the effect of the wind is taken into account in the design-orientation of the tanks. Khezri *et al.* (2012) performed experiments in a pilot-scale settling tank to determine the effect of the orientation of the tank in respect to the wind direction and velocities ranging from 2.5 to 7.0 m/s on the tank's efficiency and drew the following conclusions: (i) with increasing co-current wind velocity to 4.5 m/s, 5.5 m/s, and 7.0 m/s, the turbidity efficiency of the tank (61.24%) decreases to 50.01%, 46.04%, and 45.03%, respectively; (ii) for counter-current wind velocity equal to 2.5 m/s, the efficiency increases to 65.00%, due to the increase of solids' retention time; while (iii) for counter-current wind velocity equal to 3.5 m/s and 5.0 m/s, the efficiency decreases to 55.07% and 47.00%, respectively, due to solids' re-suspension. Based on their conclusions, the proper placement of a settling tank towards the wind could increase its efficiency by approximately 6%.

Despite its importance, the research dealing with the effect of the wind in the literature is very limited and mainly computational. Sivakumar & Lowe (1990) investigated the wind effect using a 2-D model, the k-ε turbulence model (Rodi 1980) and the sediment transport equations; they applied their model on a rectangular pilot settling tank for various wind velocities and concluded that: (i) the wind effect on the tank's flow and *SS* concentration fields is detrimental since extended re-circulation areas are created due to wind action which lead to intense mixing and uniform distribution of the *SS*; (ii) as the wind velocity increases the length of the re-circulation areas also increase while the efficiency of the tank decreases; and (iii) the wind action should be taken into consideration in the design procedure of settling tanks. Stamou & Gkesouli (2015) applied a 3-D computational fluid dynamics (CFD) model on the settling tanks of the WTP of Aharnes (WTPA) to investigate the effect of a strong (15 m/s) co-current wind on their hydraulic and settling performance; the wind was modeled via a constant horizontal flow velocity on the water surface. The results showed that the wind effect on the flow pattern and the hydraulic efficiency was strong; the wind action caused the creation of massive re-circulation areas, which covered the biggest part of the tank, intense mixing, and high short-circuiting. However, the wind effect on the removal efficiency was not pronounced; for an overflow rate, which is defined as the tank's inlet flow rate divided by its surface area, equal to $OR = 0.85$ m/h, the tank's efficiency was reduced by approximately 4.5%. Gkesouli *et al.* (2016) carried out a computational study with a 2-D CFD model, which employed the volume of fluid (VOF) method and the sediment scour model, to evaluate the wind effect of various co-current and counter-current wind velocities of up to 7.5 m/s on a rectangular settling tank for two modes of tank's operation: when the sludge removal mechanism (a) was in operation and (b) when it was out of operation. The results showed that in both modes the effect of wind

Downloaded from http://iwaponline.com/jh/article-pdf/21/1/123/658230/jh0210123.pdf
by guest

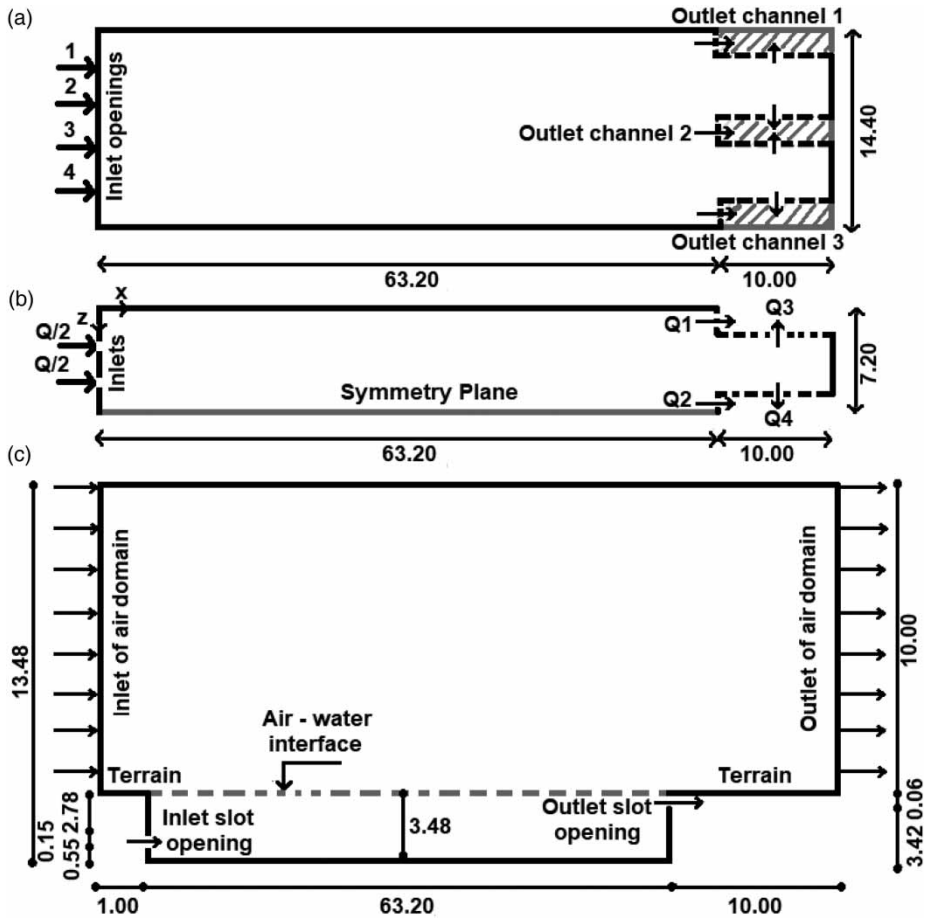

Figure 1 | Top view of (a) the tank, (b) the modeled 'half tank' and (c) the computational domain for 2-D and two-phase calculations (dimensions in m).

on the flow and *SS* concentration fields is significant; in the case of wind a two-layer flow is developed, in which the surface layer follows the wind direction, and the *SS* distributions are more uniform due to a high degree of mixing. However, the wind effect on the efficiency is minor since it is approximately equal to 1%, when the sludge scraper is in operation, and 1.3%, when the scraper is out of operation; this effect is negative in the case of co-current winds, i.e., the efficiency decreases, while for counter-current winds it is enhancing, i.e., the efficiency increases.

In this work, we extend the work of Stamou & Gkesouli (2015) to answer two research questions that are usually posed by researchers and managers: 'Is the effect of wind on settling tanks important?' and 'How can we determine this effect in our settling tanks?' To answer these questions, we propose a systematic three-step procedure that combines computational fluid dynamics modeling and experimental work, which we apply to the settling tanks of the WTPA, which is one of the most important components of the water supply system of Athens that provides water of excellent quality to 60% of the region of Attica (EYDAP SA; https://www.eydap.gr/en/SocialResponsibility/BusinessPractice/QualityCheck/). In the first and third step of the proposed procedure, we apply the 3-D model of Stamou & Gkesouli (2015) in calm and windy conditions, respectively, after having defined in the second step of the procedure the water surface velocity – wind boundary condition via 2-D and two-phase (air-water) calculations. We perform calculations for both steady and transient windy conditions and various combinations of flow rates and wind velocities and compare our results with field data; this investigation, that involves both experimental and computational work, is the first in the international literature and the main novelty of the present work.

Downloaded from http://iwaponline.com/jh/article-pdf/21/1/123/658230/jh0210123.pdf
by guest

EXPERIMENTAL

There are 16 identical rectangular settling tanks in the WTPA; the top view of one tank is shown in Figure 1(a). Water from flocculation tanks enters into the tanks via four inlet openings and exits via a series of V-notch weirs at the three outlet channels; more details can be found in Stamou & Gkesouli (2015).

Turbidity and concentration measurements

In the period October 2014–May 2015, when aluminum sulfate and PACL (polyaluminum chloride) were used as coagulants, we recorded every 5 minutes the turbidity (*NTU*) at the inlet and outlet of the tank with online turbidimeters; then, using simple averaging, we calculated the daily values only for the period with aluminum sulfate. To translate *NTU* values to *SS* concentrations (in mg/L), we measured the turbidity and *SS* concentration at various locations of the tank with a Hach 2100*N* turbidimeter and method 2540D (APHA *et al.* 2005), respectively, and we derived Equation (1).

$$SS = 1.29 \cdot NTU - 0.35 \quad (1)$$

Using Equation (1) and simple averaging, we derived the temporal variation of daily *SS* concentrations at the inlet and outlet of the tank. Based on these time series, which are plotted in Figure 2(a), we determined the average *SS* concentrations at the inlet and outlet equal to 5.7 ± 1.9 and 1.2 ± 0.6 mg/L, respectively, from which we derived the average value of the tank's efficiency equal to $R = 78.9 \pm 8.1\%$.

To model efficiently the performance of the settling tank, we had to determine a certain number of *SS* classes at its inlet (Stamou *et al.* 1989). For this reason, we measured the *SS* concentrations at the tank's inlet and classified them into four classes: C_1, C_2, C_3, and C_4; we selected this number of classes after extensive preliminary laboratory measurements starting with seven filters. For each class, we applied the filtration method 2540D (APHA *et al.* 2005) to determine its percentage in the mixture, as shown in Table 1, together with the characteristics of each class; the settling velocity is calculated using Stokes' law.

For the verification of the model, we performed *in situ* measurements of turbidity at various positions on the 15 December 2014 throughout the tank; we translated these *NTU* values into *SS* concentrations via Equation (1) and we compared them with model predictions. During this period, the wind was weak (0.6 ± 0.5 m/s), the inlet flow rate of the 16 tanks was equal to $Q = 4.3$ m^3/s, the inlet *SS* concentration was equal to 9.2 ± 7.5 mg/L, the outlet *SS* concentration was equal to 1.2 ± 0.2 mg/L, while the corresponding average efficiency was equal to $R = 86.0 \pm 1.0\%$. Moreover, we observed visually the length of the recirculation region at the water surface of the tank, which ranged from 25 m near the symmetry plane to approximately 45 m near the wall.

Wind measurements

Since the scope of the work was to assess the effect of the wind, we measured wind velocity (U_w) and direction in the

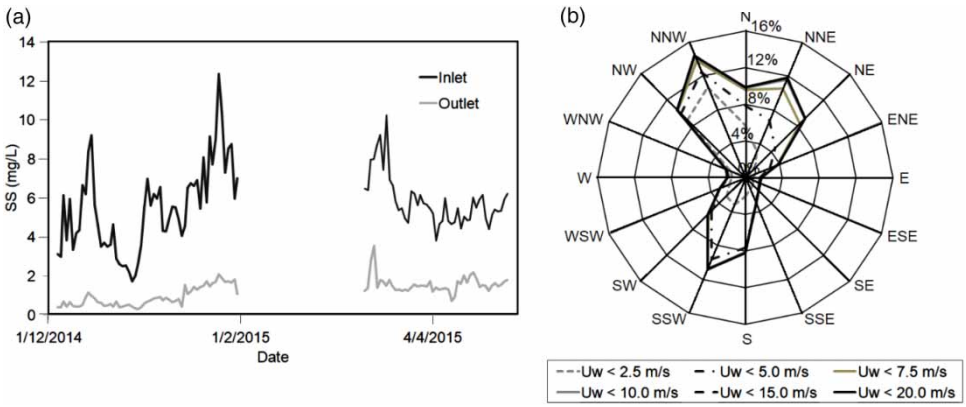

Figure 2 | (a) Daily average *SS* concentration at the inlet and outlet of the tank and (b) wind rose.

Downloaded from http://iwaponline.com/jh/article-pdf/21/1/123/658230/jh0210123.pdf
by guest

Table 1 | Characteristics of the *SS* at the tank's inlet and calculated removal efficiency

Class (–)	Range of *SS* diameter (μm)	Average diameter (μm)	Percentage (%)	Settling velocity (m/h)	*Ha* (–)	S_{in} (mg/L)	Calm conditions *R* (%)	Windy conditions *R* (%)	Ideal conditions *R* (%)
C_1	>22.5	41.0	70.0	5.80	6.32	6.4	100.0	98.0	100.0
C_2	11.0–22.5	17.0	20.5	0.96	1.04	1.9	65.6	57.5	100.0
C_3	8.0–11.0	9.5	4.0	0.31	0.34	0.4	28.5	26.6	33.5
C_4	2.5–8.0	5.0	5.5	0.09	0.10	0.5	9.7	9.5	10.2
Sum	–	–	100.0	–	–	9.2	85.1	82.0	92.4

period October 2012–May 2015 with a RNRG 40C anemometer and a 200P sensor, respectively, which were installed near the inlet of the tank at a height equal to 2.5 m from the water surface. From the distribution of the winds that is shown in the wind rose of Figure 2(b), we note that the prevailing winds originate from the north (NW, NNW, N, NNE, and NE), i.e., they are co-current with the main direction of the flow in the tank, with a total frequency equal to 55.7%; these winds may reach values up to 16.2 m/s, while the corresponding frequencies for the strong velocities of 10 and 15 m/s are equal to 2.7% and 0.4%, respectively. Generally, the effect of co-current winds on the tank's performance is expected to be negative, while that of counter-current is opposite (Gkesouli *et al.* 2016).

Turbidity measurements under strong windy conditions

In the period October 2014–May 2015, we identified three periods of strong northerly winds: 21–22 December 2014, 30–31 December 2014, and 12 January 2015. During these periods, we monitored the temporal variations of wind velocity and turbidity at the inlet and outlet of the tank as shown in Figure 3, where t is the time and $t = t_0$ is the time at which the wind velocity starts to be significant (8–10 m/s).

NUMERICAL

Equations of the model, numerical and calculation details

We applied the algebraic slip model that is virtually a simplified variation of the drift flux model by Ishii (1975), which assumes a continuous medium-mixture that is the water in the settling tanks with a dispersed phase component that is the *SS*. This mixture behaves as a single fluid and generally its density can be affected by the presence of *SS* at any point of the mixture. In the present work, we classified the *SS* of density equal to 2,730 kg/m^3 into four classes (see Table 1); each class of solids is modeled by a mass balance equation which allows a relative movement (phase slip) between the solids and the continuous medium (water) that is the settling. To determine the 3-D flow field in the settling tanks, we solved the bulk continuity and momentum equations which are formed by summing the corresponding equations over both phases and classes (ANSYS-CFX 2018) and the SST k-omega turbulence model. More information on the equations of the model and the numerical code can be found in ANSYS-CFX (2018) and Stamou & Gkesouli (2015).

The settling tanks, whose simplified top view is shown in Figure 1(a), are approximately symmetrical; therefore, we decided to model the left half of the tank, which is shown in Figure 1(b), assuming symmetry on a plane xy in the middle of the tank. This approach has been used in cases of relatively symmetrical flows to reduce the total computational effort. Then, we defined the boundary conditions at the borders of the calculation domain. At the two inlet openings, a parallel flow was imposed with uniform horizontal velocity, vertical velocity equal to zero and medium turbulent intensity equal to 5% while the solids' concentration was assumed to be uniformly distributed with concentration equal to S_{in}. At the two outlet channels the 'opening' boundary condition was used that allows the water to enter or exit the tank and the pressure was set equal to zero, while the gradients of *SS*, k, and ω at the outlet channels were set equal to zero. The vertical walls

Downloaded from http://iwaponline.com/jh/article-pdf/21/1/123/658230/jh0210123.pdf
by guest

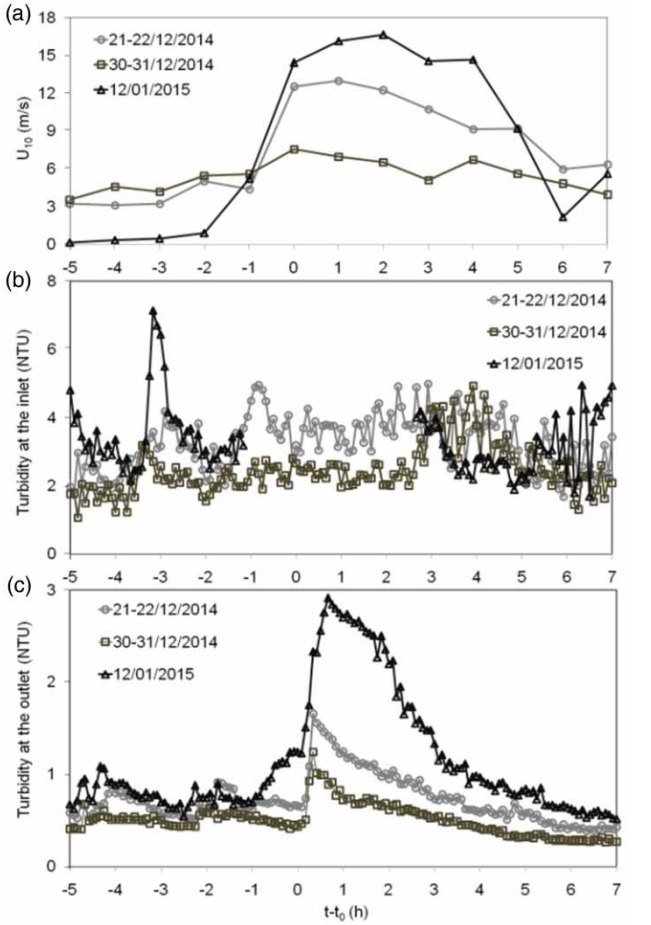

Figure 3 | (a) Wind velocity, (b) turbidity at the tank's inlet, and (c) turbidity at the tank's outlet under strong windy conditions.

were treated as no slip–smooth wall boundaries with the exception of the right side of the tank, at which, the symmetry condition was used. At the bottom, which was treated as a smooth wall, the solids were assumed to be deposited and removed from the computational domain, i.e., the formation of sludge layer was not taken into account. The free surface was treated as a free slip wall; accordingly, the normal velocity component and the normal gradients of all other variables were set equal to zero. The modeling of the wind effect is described in the section 'Proposed modeling procedure to assess the effect of the wind'. The computational grid consisted of approximately 127,000 elements with dimensions ranging from 1 to 30 cm and approximately 472,000 nodes; this grid size was selected after a series of preliminary calculations that verified grid independence.

Proposed modeling procedure to assess the effect of the wind

To examine the effect of the wind, we propose a modeling procedure, which consists of the following three steps.

Step 1

We perform calculations in calm conditions to determine the 3-D hydrodynamic characteristics of the tank and its removal efficiency, after selecting the proper grid that ensures grid independence. When measurements are available, these can be used for model calibration and/or verification. It is noted, however, that the hydrodynamic model does not commonly contain parameters or coefficients that can be tuned; typically, the only two calibration possibilities are the value of the Schmidt number or the portions of the *SS* classes (Stamou & Gkesouli 2015). When no measurements are available, which is typically the case in tanks in the design phase, we may use a model that has been verified in similar tanks and conditions.

Step 2

Ideally, the second step is to use a 3-D and three-phase (air–water–solids) model to perform simulations that take into account the effect of the wind. Practically, a single run of such calculation, even using relatively simple, but effective turbulent models may require a few months with normal PCs (e.g., an Intel Core i7–3.33 GHz desktop) (Gkesouli & Stamou 2017). An alternative, but more economical and faster approach is to determine a typical value of the flow velocity at the water surface and set it as a boundary condition along the water surface. This 'surface velocity' U_s, is expected to depend on the velocity of the wind that is usually defined at a height of 10 m (U_{10}). The easiest way to determine values of this velocity is directly from the experience from coastal modeling. In the present case, we applied a more rational and accurate approach to derive such values after performing a series of calculations using the model in its 2-D and two-phase (air–water) formulation; a view of the computational domain is shown in Figure 1(c). Based on these calculations, we found that the variation of U_s with distance from the beginning of the tank ($x = 0$) is

Downloaded from http://iwaponline.com/jh/article-pdf/21/1/123/658230/jh0210123.pdf
by guest

expressed satisfactorily (correlation coefficient = $r^2 = 0.949$) by Equation (2).

$$U_s/U_{10} = 0.005 \ln(x) + 0.002 \quad (2)$$

Equation (2) shows that U_s increases with increasing x until $x = 25$ m, while for $x > 25$ m it is approximately constant and equal to 2.3% of U_{10}; this value is within the range of values encountered in the literature (0.9–5.8%) for coastal waters, lakes, and reservoirs (see, for example, Wu 1983).

Step 3

We apply the constant value of 2.3% of U_{10} as a boundary condition at the water surface and we perform 3-D and two-phase (water–*SS*) calculations to examine the effect of the wind. However, these calculations should be performed not only for steady, but also for transient conditions, which are expected to produce less conservative results according to the performed experiments (see Figure 3(c)).

RESULTS AND DISCUSSION

Calculations in calm conditions

To verify the model, we performed calculations in calm conditions: (a) for steady-state flow and constant inlet *SS* concentration (24 hours daily average, 15 December 2014) and (b) for transient conditions and variable inlet *SS* concentration (from 4:00 to 8:00 of the 22 December). In steady-state conditions, Figure 4 depicts that the flow field is 3-D and very complex, being characterized by the formation of a main anti-clockwise re-circulation region (eddy V1), which is created due to the incoming jets from the two inlet openings. Its length ranges from about 47 m near the solid wall (see Figure 4(b)) to about 20 m near the symmetry plane (see Figure 4(c)); these values are in satisfactory agreement with the respective observed values (i.e., 45 to 25 m). Moreover, Figure 4(a) and 4(d) indicate a satisfactory agreement between the calculated *SS* concentrations (denoted by contours) with measurements (denoted by circles) in the tank, outside the region of eddy V1; however, in the eddy, the calculated *SS* concentrations are lower than measurements. This behavior was expected, since in the real tank, mixing in the eddy is intense and causes solids' re-suspension of the sludge layer that results in very high *SS* concentrations in this area. The formation of the sludge layer and the process of solids' re-suspension are not taken into account by the present model. However, this does not affect the capability of the model to predict satisfactorily the solids' removal efficiency of the tank, which was calculated equal to 85.1%, as shown in Table 1, depicting a very good agreement with the measured value (86.0 ± 1.0%). It is mentioned that the present 3-D model has also been verified successfully in the same tank, when the scraper mechanism was not in operation and the removal efficiency ranged from 67 to 72% (Stamou & Gkesouli 2015). Figure 5 illustrates that the calculated removal efficiencies for transient conditions are in satisfactory agreement with the respective experimental values, thus showing that the model predicts successfully the tank's behavior for variable *SS* inlet concentrations.

After the verification of the model, we applied the model for 36 combinations of flow rates and settling velocities to determine the curve $1 - R$ versus Hazen number (*Ha*) that is shown in Figure 6, which is expressed by Equation (3) ($r^2 = 0.995$); it is noted that *Ha* number is defined as the solids' settling velocity divided by the tank's overflow rate (*OR*).

$$1 - R = \exp^{-1.087Ha} \quad (3)$$

Figure 6 is of great practical importance because it can be used to determine the efficiency of the tank for various combinations of *OR* and settling velocities without any CFD computations. Moreover, we determined the percentages of flow (% of *Q*) exiting the tank via the four outlet weirs that are shown in Table 2. These percentages do not depend on the flow rate while the weir loading is the same in all weirs and ranges from 371 to 764 m^3/d per m.

Calculations in windy steady-state conditions

We performed steady-state calculations for the maximum wind velocity $U_{10} \approx 20$ m/s. Figure 7 shows that when the

Downloaded from http://iwaponline.com/jh/article-pdf/21/1/123/658230/jh0210123.pdf
by guest

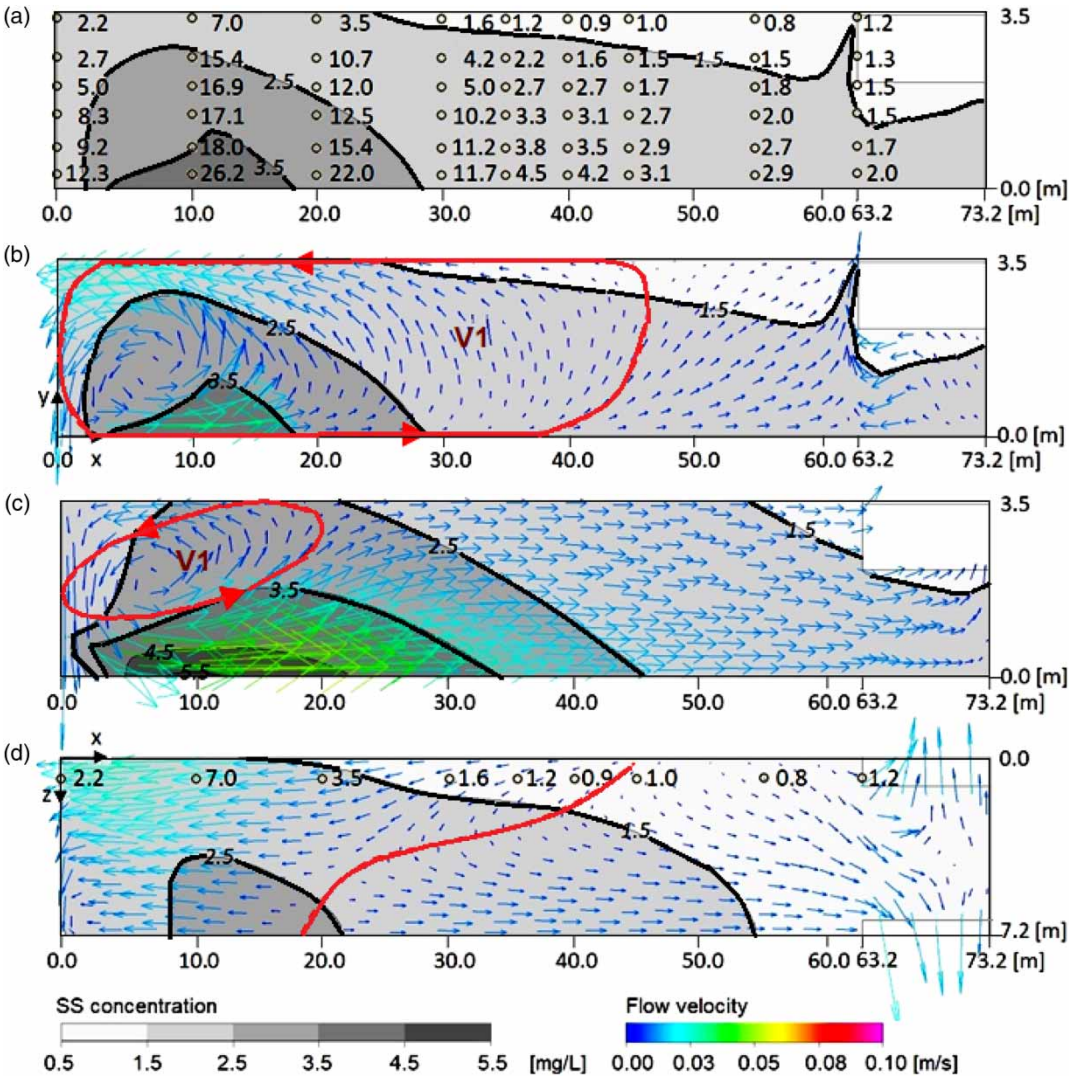

Figure 4 | *SS* concentrations and flow velocities: (a) and (b) on a vertical plane near the wall, (c) on a vertical plane near the symmetry plane, and (d) on a horizontal plane near the surface; the numbers denote measured values and the contours denote computations.

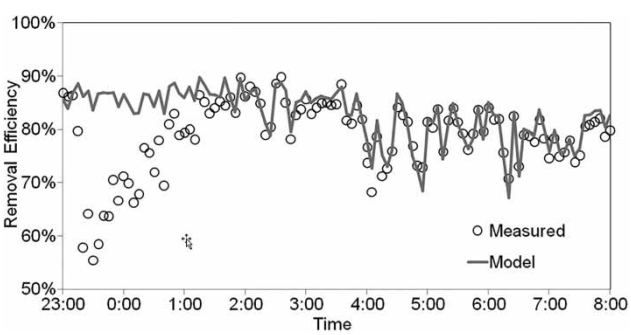

Figure 5 | Comparison of calculated removal efficiency vs. experimental.

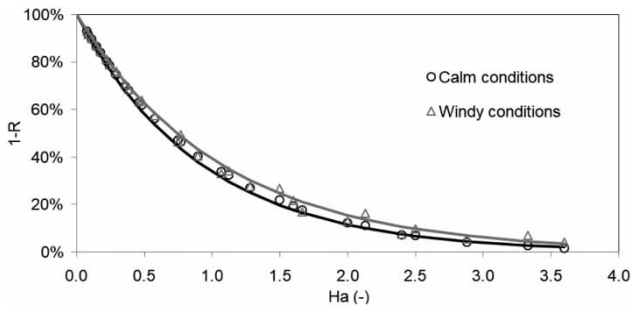

Figure 6 | Efficiency curve (1 – *R*) versus Hazen number (*Ha*) for calm and windy conditions.

Downloaded from http://iwaponline.com/jh/article-pdf/21/1/123/658230/jh0210123.pdf
by guest

Table 2 | Outlet flow rates (% of Q) and weir loadings

		Calm conditions		Windy conditions		Calm conditions		Windy conditions	
		Flow rate (%)		Flow rate (%)		Weir loading (m^3/m.d)		Weir loading (m^3/m.d)	
Outlet weir (–)	Weir length (m)	$Q = 3$ m^3/s	$Q = 6$ m^3/s	$Q = 3$ m^3/s	$Q = 6$ m^3/s	$Q = 3$ m^3/s	$Q = 6$ m^3/s	$Q = 3$ m^3/s	$Q = 6$ m^3/s
1	1.15	5.3	5.3	9.6	6.6	375	749	674	930
2	0.62	2.9	2.9	7.2	4.7	382	764	943	1214
3	10.00	45.9	45.9	43.0	45.1	371	743	349	731
4	10.00	45.9	45.9	40.2	43.6	372	744	325	706
Sum	21.77	100.0	100.0	100.0	100.0	–	–	–	–

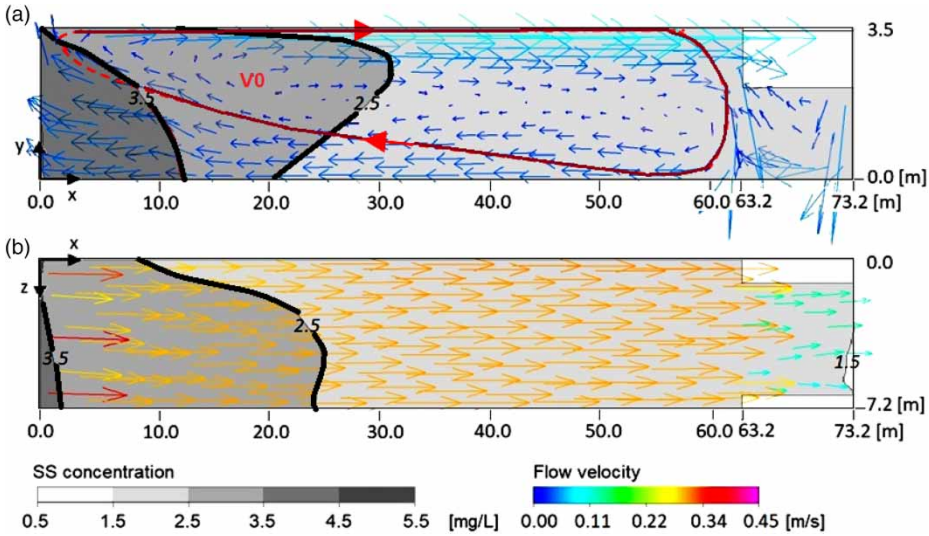

Figure 7 | Calculated *SS* concentrations and flow velocities in windy steady-state conditions on (a) a vertical plane near the wall and (b) a horizontal plane near the surface.

wind is present the degree of complexity and three-dimensionality of the flow is reduced; a massive clockwise eddy V0, which practically covers the whole tank is created that results in intense mixing and more uniform distribution of all quantities. The *SS* iso-concentration lines become more vertical in comparison with the no-wind case (see Figure 4), and they are shifted upwards and towards the surface and the outlet. Subsequently, the *SS* concentrations increase and the removal efficiency decreases to 82.0% (see Table 1).

Moreover, we carried out 36 series of additional calculations for various combinations of flow rates (3–6 m^3/s) and *Ha* (0.11–3.50) to determine Equation (4) ($r^2 = 0.979$) that is compared in Figure 6 with the no-wind case; see Equation (3). As expected, the presence of the wind results in decrease of the tank's efficiency.

$$1 - R = \exp^{-0.936Ha} \tag{4}$$

In Figure 8(a) and 8(b), the curve $1 - R$ vs. *Ha* is shown for various flow rates and wind velocities, respectively; Figure 8(a) and 8(b) show clearly that the effect of co-current wind on the removal efficiency increases with increasing wind velocity, increasing *Ha* and decreasing *OR*, i.e., the effect of wind is suppressed by high flow rates.

In Table 2 the percentages of flow rate (Q_1/Q, Q_2/Q, Q_3/Q, and Q_4/Q) exiting the tank via the four outlets for the maximum wind velocity ($U_{10} = 20$ m/s) are compared

Downloaded from http://iwaponline.com/jh/article-pdf/21/1/123/658230/jh0210123.pdf
by guest

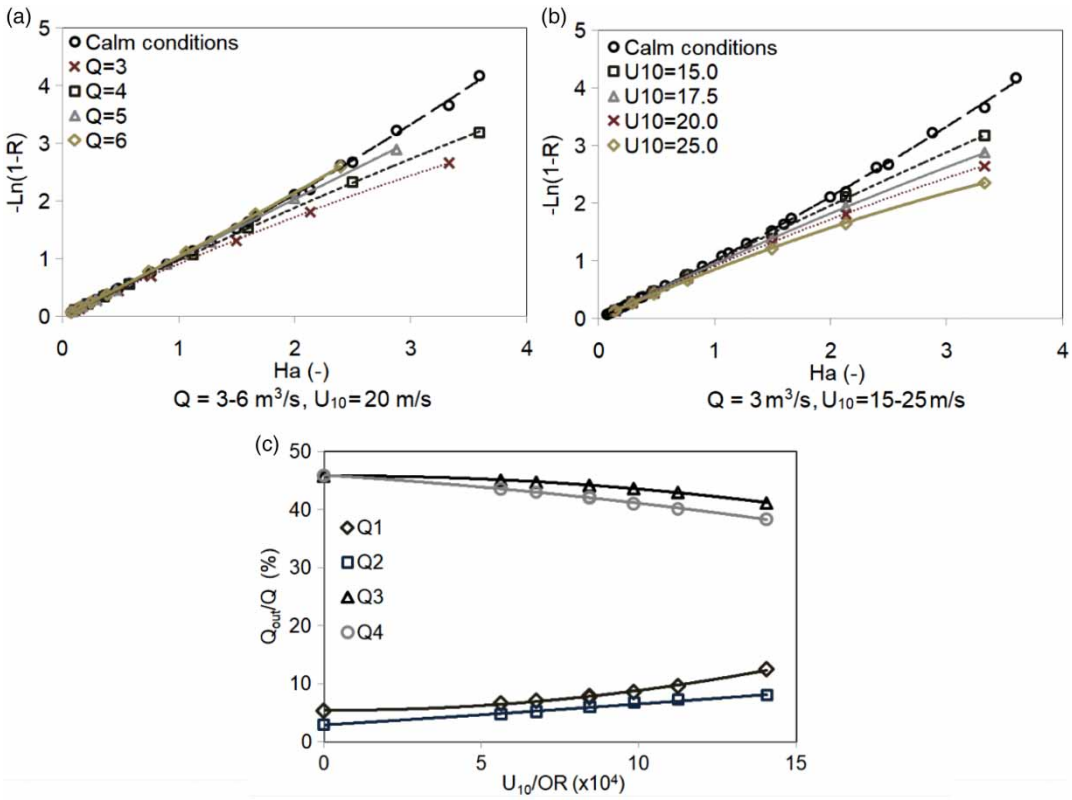

Figure 8 | (a) Efficiency curve $(1 - R)$ vs. Hazen number *(Ha)* for various flow rates (3–6 m^3/s); (b) efficiency curve $(1 - R)$ versus Hazen number *(Ha)* for various wind velocities (15–25 m/s); (c) outlet flow rates vs. U_{10}/OR.

with the corresponding values for calm conditions, while in Figure 8(c) these percentages are plotted vs. U_{10}/OR for various flow rates (3–6 m^3/s) and wind velocities (15–25 m/s). Table 2 and Figure 8(c) depict that the percentages of flow exiting via the outlets 1 and 2 increase significantly when U_{10}/OR increases, while the outflows via outlets 3 and 4 decrease. The behavior of weir loadings is similar; they increase dramatically (up to 1.5 times) at the outlets 1 and 2, and decrease up to 13% at the outlets 3 and 4. The *SS* concentrations increase at all outlets, when U_{10}/OR increases; this increase is higher at the central outlets 2 and 4 in comparison with the outlets 1 and 3 near the wall.

Calculations in windy transient conditions

Generally, it is extremely difficult to standardize the behavior of the wind velocity; however, for the purpose of modeling we identified three stages that are shown in Figure 9(a). In the first stage, wind velocity increases within 1 hour practically linearly from an initial value $U_{10,0}$ to a very high value of about 8–10 m/s and then reaches its maximum value $U_{10,max}$. In the second stage, wind velocity remains approximately constant around its maximum value for about 2–5 hours, and in the third stage it drops to its final value $U_{10,end}$ following approximately a linear line. Figure 9(a) shows that the turbidity at the tank's outlet exhibits similar behavior. In the first stage, turbidity starts (at $t = t_0$) to increase linearly with time from its initial value NTU_0 to a maximum value NTU_{max} within 20–40 min ($t = t_{max}$). Then, in the second stage it remains around its maximum value for a short period until the start of the third stage, where *NTU* decreases exponentially with a decay coefficient (k_d) as shown by Equation (5), to reach its final value (NTU_{end}). The values of these behavior characteristics are shown in Table 3. The measured behavior of the wind and the turbidity at the outlet is depicted in Figure 9(b), while its characteristics are shown in Table 3; generally, the

Downloaded from http://iwaponline.com/jh/article-pdf/21/1/123/658230/jh0210123.pdf
by guest

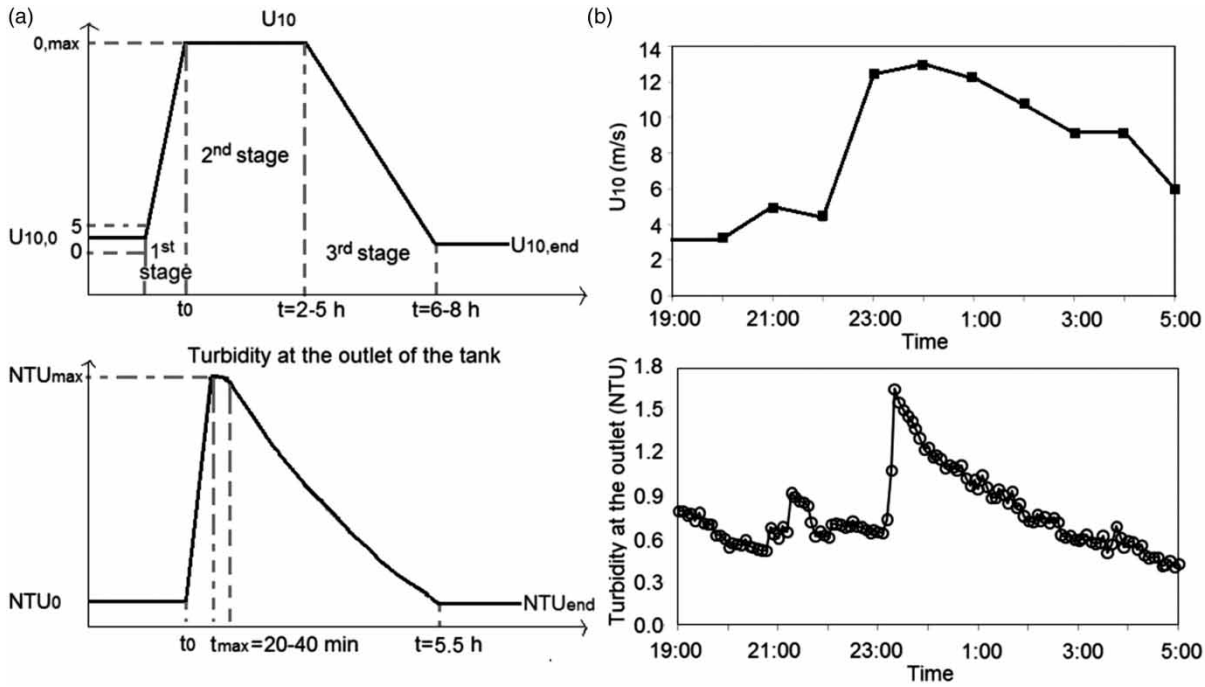

Figure 9 | Variation of the wind velocity and the turbidity at the outlet of the tank; (a) typical behavior and (b) measured values (21–22 December 2014).

Table 3 | Characteristics of the behavior of the tank for transient windy conditions

Parameter	Units	Typical	21–22 December 2014
$U_{10,0}$	m/s	0.0–5.0	4.4
Slope $U_{10,0} -> U_{10,max}$	m/s^2	0.0023–0.0026	0.0023
$U_{10,max}$	m/s	12.0–17.0	12.5–13.0
Slope $U_{10,max} -> U_{10,end}$	m/s^2	0.0008–0.0012	0.0008
$U_{10,end}$	m/s	2.0–6.0	6.0
NTU_0	NTU	0.40–0.70	0.65
Slope $NTU_0 -> NTU_{max}$	NTU/s	0.0005–0.0007	0.0005
NTU_{max}	NTU	1.20–2.92	1.65
NTU_{max}/NTU_0	–	2.2–4.0	2.5
k_d	1/h	0.24–0.33	0.24
NTU_{end}	NTU	0.30–0.90	0.50

behavior during this incident follows the typical pattern of Figure 9(a).

$$NTU = NTU_{\max}/NTU_0 \exp^{-kd(t-tmax)} \quad (5)$$

We performed transient calculations to determine the tank's efficiency for the conditions of the 5-hours' strong wind incident of 21–22 December 2014, from 23:00 until 4:00, which is shown in Figure 5 together with the measured values. During these calculations, the wind and the turbidity at the inlet were set equal to their measured values, which are shown in Figures 9(b) and 3(b), respectively. Figure 5 shows that in the first half hour (23:00–23:30) the tank's efficiency decreases to approximately 55% and then it increases progressively to reach its steady-state high values of about 83% at 1:30. The model does not capture the decline of efficiency during this 2.5-hour period showing practically no sensitivity to the increase of the wind velocity. However, from 1:30 until 4:00, the calculated efficiency is very close to the measured and thus the model performs very well. Moreover, after 4:00, when the wind velocity is not strong and its effect can practically be ignored, the performance of the model is also very good (see Figure 5). The unsatisfactory prediction of the model during the period 23:00–1.30 is due to the fact that the present model cannot take into account the effect of the sludge layer and the subsequent re-suspension of the settled solids. In the real tank, the

Downloaded from http://iwaponline.com/jh/article-pdf/21/1/123/658230/jh0210123.pdf
by guest

solids that settle on the bottom form a sludge layer of a height around 15–20 cm; the settled solids may re-suspend due to the effect of the eddy V1 in calm conditions (see Figure 4) or the eddy V0 in windy conditions (see Figure 7). Figure 10 shows the temporal variation of the flow field from the steady-state calm conditions to the windy conditions with the corresponding times and efficiencies. Figure 10 illustrates clearly that in the initial period the transient flow field 'pushes' the solids contained in the eddy V1 towards the outlet. The *SS* concentrations in the eddy V1 are much higher in the real tank, due to the effect of the sludge layer and the subsequent re-suspension, and thus their effect on the efficiency is more pronounced than that predicted by the model. Therefore, to increase the predictive accuracy of the model in transient conditions, we need to model the effect of the sludge layer and the subsequent re-suspension.

CONCLUSIONS

We presented a systematic procedure that involves computational fluid dynamics modeling and experimental work to answer the research questions that are usually posed by researchers and managers of water treatment plants 'Is the effect of wind on settling tanks important?' and 'How can we determine this effect in our settling tanks?' Then, we apply this procedure in the water treatment plant of Aharnes, Athens to derive the following conclusions. (1) The effect of wind increases with increasing co-current wind velocity, increasing settling velocity and decreasing flow rate. (2) In windy steady-state flow conditions, the degree of complexity and three-dimensionality of the flow field that is observed in calm conditions is reduced and the removal efficiency decreases from 85.1 in calm conditions to 82.0%. Predicted efficiencies for constant and variable inlet solids' concentrations compare favorably with measurements. (3) In windy, transient flow conditions, the effect of wind on the efficiency of the tank can be very pronounced. Within the first half hour of the windy period the efficiency decreases to approximately 55%; the present model does not capture this effect, because it cannot simulate the sludge layer and the subsequent re-suspension of the settled solids. Such a simulation is an important research challenge. The above-mentioned remarks illustrate the need for the managers of water treatment plants to apply the proposed procedure to determine the effect of the wind on their settling tanks and on all types of tanks and reactors of their plants as well. Moreover, they show that the placement of rectangular tanks co-currently to the prevailing wind direction should be avoided.

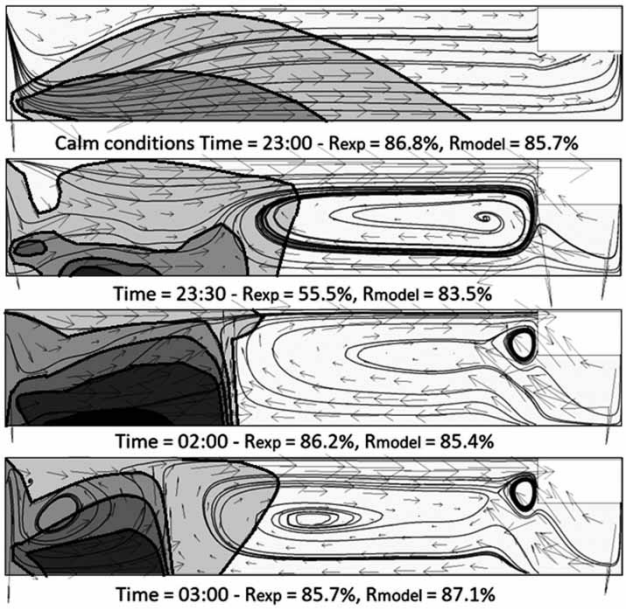

Figure 10 | Temporal variation of the flow field on a vertical plane near the symmetry plane during the wind incident of the 21–22 December 2014.

ACKNOWLEDGEMENTS

The present work was performed in the National Technical University of Athens (NTUA) within the framework of two research projects; the financial support provided by Athens Water Supply and Sewerage Company EYDAP SA is gratefully acknowledged. Furthermore, the authors would like to thank the personnel of EYDAP SA for the useful discussions and for the provision of the required information and data, especially Mr A. Magoulas, Mrs M. Xanthaki, Mrs A. Synodinou, Dr F. Miskaki, Dr N. Defteraios, Dr T. Kaloudis, Dr E. Smeti, Mrs R. Polomarkaki, Mr G. Dimtsas, and Mrs M. Spanakou. Moreover, the authors would like to thank Prof. D. Mamais and the personnel of the Laboratory of Sanitary Engineering of the NTUA.

Downloaded from http://iwaponline.com/jh/article-pdf/21/1/123/658230/jh0210123.pdf
by guest

REFERENCES

Aalderlink, R. H., Lijklema, L., Breukelmam, J., Raaphorst, W. V. & Brinkman, A. G. 1984 Quantification of wind induced resuspension in a shallow lake. *Water Science and Technology* **17** (6–7), 903–914.

Abdel-Gawad, S. M. & McCorquodale, J. A. 1985 Numerical simulation of rectangular settling tanks. *Journal of Hydraulic Research* **23** (2), 85–100. https://doi.org/10.1080/00221688509499358.

Al-Sammarraee, M. & Chan, A. 2009 Large-eddy simulations of particle sedimentation in a longitudinal sedimentation basin of a water treatment plant. Part 2: the effects of baffles. *Chemical Engineering Journal* **152**, 315–321. https://doi.org/10.1016/j.cej.2009.01.052.

ANSYS-CFX 2018 http://www.ANSYS.com (accessed 16 April 2018).

APHA, AWWA & WEF 2005 *Standard Methods for the Examination of Water and Wastewater*, 21st edn. American Public Health Association (APHA)/American Water Works Association (AWWA)/Water Environment Federation (WEF), Washington, DC, USA.

Crittenden, J. C., Trussell, R. R., Hand, D. W., Howe, K. J. & Tchobanoglous, G. 2012 *MWH's Water Treatment: Principles and Design*, 3rd edn. John Wiley and Sons, Hoboken, NJ.

Deininger, A., Holthausen, E. & Wilderer, P. A. 1998 Velocity and solids distribution in circular secondary clarifiers: full scale measurements and numerical modelling. *Water Research* **32** (10), 2951–2958. https://doi.org/10.1016/S0043-1354(98)00072-4.

Ekama, G. A. & Marais, P. 2004 Assessing the applicability of the 1D flux theory to full-scale secondary settling tank design with a 2D hydrodynamic model. *Water Research* **38**, 495–506. https://doi.org/10.1016/j.watres.2003.10.026.

EYDAP SA https://www.eydap.gr/en/SocialResponsibility/BusinessPractice/QualityCheck/ (accessed 30 April 2018).

Florida Rural Water Association 2005 *Water Treatment Process Troubleshooting Guide for Class A and Class B Operators, Supplement to Small Water Systems Training Manual*. http://www.frwa.net/uploads/4/2/3/5/42359811/a&boperatorscertificationmanual120611.pdf (accessed 14 April 2018).

Gkesouli, A. & Stamou, A. 2017 CFD modelling of wind effect on rectangular settling tanks of water treatment plants. *European Water* **58**, 61–67. http://www.ewra.net/ew/pdf/EW_2017_58_10.pdf (accessed 14 April 2018).

Gkesouli, A., Nitsa, M., Stamou, A., Rutschmann, P. & Bui, M. D. 2016 Modeling the effect of wind in rectangular settling tanks for water supply. *Desalination and Water Treatment* **57** (54), 26345–26354. https://doi.org/10.1080/19443994.2016.1195290.

Goula, A. M., Kostoglou, M., Karapantsios, T. D. & Zouboulis, A. I. 2008 A CFD methodology for the design of sedimentation tanks in potable water treatment: case study: the influence of a feed flow control baffle. *Chemical Engineering Journal* **140**, 110–121. https://doi.org/10.1016/j.cej.2007.09.022.

Ishii, M. 1975 *Thermo-fluid Dynamic Theory of Two-Phase Flow. Collection de la Direction des Etudes et Researches de EDF*. Eyrolles, Paris, 22, France.

Jover-Smet, M., Martin-Pascual, J. & Trapo, A. 2017 Model of suspended solids removal in the primary sedimentation tanks for the treatment of urban wastewater. *Water* **9** (6), 448. https://doi.org/10.3390/w9060448.

Kawamura, S. 2000 *Integrated Design and Operation of Water Treatment Facilities*, 2nd edn. John Wiley and Sons, New York.

Khezri, S. M., Biati, A. & Erfani, Z. 2012 Determination of the effect of wind velocity and direction changes on turbidity removal in rectangular sedimentation tanks. *Water Science and Technology* **66** (12), 2814–2820. doi: 10.2166/wst.2012.533.

Matko, T., Fawcett, N., Sharp, A. & Stephenson, T. 1996 Recent progress in the numerical modelling of wastewater sedimentation tanks. *Trans Ichem E* **74** (B), 245–258. https://doi.org/10.1205/095758296528590.

Rodi, W. 1980 *Turbulence Models and Their Application in Hydraulics – A State of the Art Review*, 3rd edn. IAHR, The Netherlands.

Sivakumar, M. & Lowe, S. A. 1990 Simulation of the effect of wind on rectangular sedimentation tanks. In: *Conference on Hydraulics in Civil Engineering*, Sydney, Australia, pp. 74–78.

Stamou, A. & Gkesouli, A. 2015 Modeling settling tanks for water treatment using computational fluid dynamics. *Journal of Hydroinformatics* **17** (5), 745–762. https://doi.org/10.2166/hydro.2015.069.

Stamou, A. I., Adams, E. A. & Rodi, W. 1989 Numerical modelling of flow and settling in primary rectangular clarifiers. *Journal of Hydraulic Research* **27** (5), 665–682. https://doi.org/10.1080/00221688909499117.

Stamou, A. I., Latsa, M. & Assimacopoulos, D. 2000 Design of two-storey final settling tanks using mathematical models. *Journal of Hydroinformatics* **2** (4), 235–245. https://doi.org/10.2166/hydro.2000.0021.

Wu, J. 1983 Sea-surface drift currents induced by wind and waves. *Journal of Physical Oceanography* **13**, 1441–1451. https://doi.org/10.1175/1520-0485(1983)013 < 1441:SSDCIB > 2.0.CO;2.

First received 9 May 2018; accepted in revised form 19 October 2018. Available online 19 November 2018

Downloaded from http://iwaponline.com/jh/article-pdf/21/1/123/658230/jh0210123.pdf
by guest